Accepted Manuscript

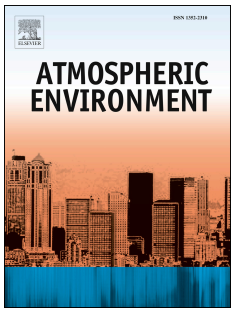

Light attenuation versus evolved carbon (AVEC) – A new way to look at elemental and organic carbon analysis

E.M.G. Nicolosi, P. Quincey, A. Font, G.W. Fuller

PII: S1352-2310(17)30853-1

DOI: 10.1016/j.atmosenv.2017.12.011

Reference: AEA 15730

To appear in: *Atmospheric Environment*

Received Date: 17 March 2017

Revised Date: 27 November 2017

Accepted Date: 11 December 2017

Please cite this article as: Nicolosi, E.M.G., Quincey, P., Font, A., Fuller, G.W., Light attenuation versus evolved carbon (AVEC) – A new way to look at elemental and organic carbon analysis, *Atmospheric Environment* (2018), doi: 10.1016/j.atmosenv.2017.12.011.

Light attenuation versus evolved carbon (AVEC) – a new way to look at elemental and organic carbon analysis

E.M.G. Nicolosi[1,2*], P. Quincey[2], A. Font[1] and G.W. Fuller[1*]

[1]MRC-HPA Centre for Environment and Health, School of Biomedical & Health Sciences, King's College London, 150 Stamford Street, London SE1 9NH, UK

Chemical, Medical and Environmental Sciences Department, National Physical Laboratory, Hampton Road, Teddington, Middlesex

TW11 0LW, UK

Keywords: OCEC analysis; thermal desorption; optical attenuation; air quality; particulate matter.

* Corresponding authors. E-mail addresses: eleonora.nicolosi@kcl.ac.uk and gary.fuller@kcl.ac.uk

Postal address: King's College London, Environment Research Group, 150 Stamford Street, London SE1 9NH, United Kingdom

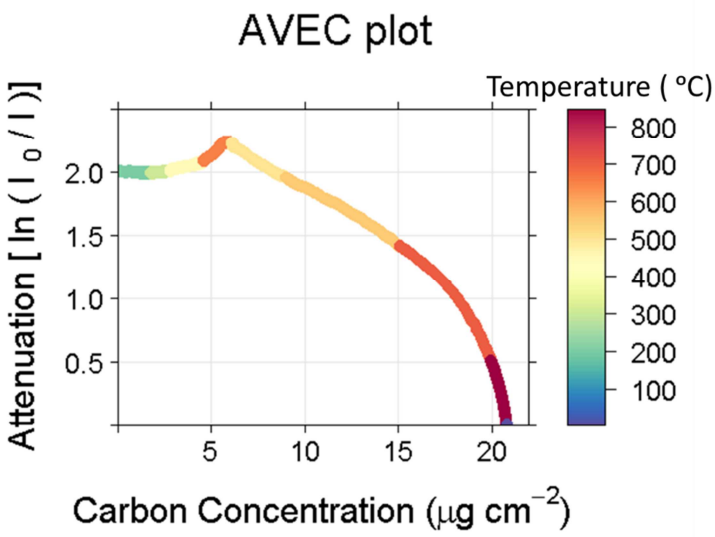

Abstract

The Attenuation Versus Evolved Carbon (AVEC) plot is a new way to represent thermal-optical organic carbon/elemental carbon (OC/EC) analysis data. The accumulated carbon concentration is plotted against the attenuation (ln (I_0/I)). Unlike the thermogram, it provides information about the sample properties rather than the instantaneous instrument sensor status.

The plot can be used to refine the determination of OC and EC split point, either from consideration of laser instability or transit time within the instrument; to investigate the optical properties of the particles; and to spot the early evolution of pyrolysed carbon (PC) and/or EC during the inert phase.

168 samples from three sites were studied. The gradient of the AVEC plot curve in the oxygenated phase provides information about the mass absorption cross section (σ) of the particles leaving the filter. The σ of the PC generated in the higher temperature Quartz protocol was greater than the PC generated in the lower temperature EUSAAR_2 protocol. Also, in both cases the PC evolved at a lower temperature in the oxygenated phase than the native EC.

To minimise the shadowing effect, σ was also measured for the particles leaving the filter at the end of the analysis. These σ values, which are expected to be a combination of inherent σ together with fixed instrumental factors, were consistent between the different sites (45 ± 10 m^2 g^{-1} in rural samples, 42 ± 8 m^2 g^{-1} in urban samples and 35 ± 14 m^2 g^{-1} in roadside samples).

The AVEC plot can be generated from the data routinely produced by the analytical instrument using the R-code supplied in the supplementary material.

1 Introduction

Elemental Carbon (EC) is an important component of our air pollution. Air pollution consists of a complex combination of gases and particulate matter (PM), the term for the mixture of solid particles and liquid droplets found in the air.

PM profoundly impacts human health (Kim et al., 2015), visibility, natural ecosystems, the weather, and the climate (IPCC, 2013). These PM effects are dependent on the aerosol properties, including the number concentration, size, and chemical composition. PM is emitted directly into the atmosphere (primary) or formed in the atmosphere through gas-to-particle conversion (secondary) (Zhang et al., 2015). Furthermore, primary and secondary PM undergoes chemical and physical transformations and is subjected to transport, cloud processing, and removal from the atmosphere.

Carbon in PM falls broadly into three categories that are defined operationally: EC, organic carbon (OC), and carbonate carbon (CC). Recently, more attention has been drawn to EC, due to its linkage to adverse health (Janssen et al., 2011, Janssen et al., 2012, Samoli et al., 2016) and climate effects (Ramanathan and Carmichael, 2008, Jacobson, 2010). Several studies suggest that EC is a valid indicator for traffic emissions and include its analysis during monitoring campaigns (Lena et al., 2002, Schauer et al., 2003, Chiappini et al., 2014, Atkinson et al., 2015, Qadir et al., 2013). A number of EC measurement techniques exists (Cachier et al., 1989, Watson et al., 2005, Hitzenberger et al., 2006) with the thermal-optical method being broadly used in Europe and the USA. Usually this follows one of three common protocols: NIOSH5040 (Birch and Cary, 1996), IMPROVE_A (Chow et al., 2007) and EUSAAR_2 (Cavalli et al., 2010).

Measurements of the OC and EC content of particulate samples collected on quartz filters are commonly made and feature in legislation such as the European Air Quality Directive [Directive 2008/50/EC]. Details of the analytical technique are given in the Methods section.

While the determination of the total amount of carbon (TC = OC + EC) in the sample is relatively well defined, it is important to realise that the split of the TC into OC and EC is a useful but ultimately convention-based process with no precisely correct values. EC is generally expected to be comparable with eBC, a measure of light-absorbing material loosely termed "soot" (Petzold et al., 2013). By convention, the OC is the carbonaceous material that is removed from the filter by heating to a defined temperature in an inert atmosphere (He), plus any carbonaceous material determined to have been pyrolysed (PC) during this phase. Optical information is used to assess the pyrolysis using a laser that measures the transmittance through the filter. EC is the remaining carbonaceous material removed during the heating of the sample in the later, oxidising atmosphere (He/O_2), phase of the measurement. The system is complicated by the presence of carbonaceous material in the form of carbonate (Karanasiou et al., 2015), and by interactions with other chemical components of the material (Fung et al., 2002).

The main aim of this paper is to present a new method of visualising the sample analysis data from thermal-optical measurements. This new method has two main advantages: it provides a more intuitive and useful visual summary of the analysis than the thermogram, which is commonly used; and it provides information about the optical properties of the material evolving from the sample during the oxidising phase of the analysis. This opens up the possibility of improved discrimination between OC and EC, using the data that are available from routine analysis. We call the new presentation of the analytical data the Attenuation Versus Carbon Evolved (AVEC) plot.

2 Methods

2.1 Sampling

Two sets of samples were analyzed in this study. First, a set was collected during the Intensive Observational Periods of the NERC-funded Clean Air for London (ClearfLo) Project (www.clearflo.ac.uk); a large, multi-institutional collaborative scientific project based in the UK. Those comprised a winter (January–February) and a summer (July–August) campaign in 2012. The sample locations were Harwell (a rural site in Oxfordshire, 85 km west of London); London North Kensington (an urban background site located in a school playground in a residential area); and London Marylebone Road (a roadside site located within 1 m of the kerbside of a busy main arterial route in central London with traffic flows of ~90,000 vehicles per day). The locations were also part of the Defra Particles Network (Butterfield et al., 2013). These samples were collected on quartz filters using a Partisol Plus 2025 operating at a flow rate of 16.7 litres min^{-1}.

The Centre for Research into Atmospheric Chemistry, University College Cork, supplied the samples of coal burning emissions that constitute the second set of samples analysed.

2.2 OC/EC analysis

OC and EC were measured by an OCEC Sunset laboratory thermal/optical analyser (Birch and Cary, 1996) using the EUSAAR_2 protocol (Cavalli et al., 2010) and a modified version of the NIOSH protocol, Quartz. The parameters of the two protocols can be found in the supplementary material, Table 1.

The analysis procedure was the following: after the sample was placed in the main oven, the temperature was increased from the laboratory temperature to the one stated in the chosen protocol. At the same time helium (He) was supplied into the sample chamber. The inert atmosphere and the increasing temperature allowed OC to leave the filter and move towards the manganese dioxide (oxidising) oven. This consisted of a manganese dioxide catalyst that converted OC to carbon dioxide (CO_2) at 840°C. CO_2 was then reduced to methane (CH_4) by a heated nickel catalyst. The CH_4 passed through a flame ionisation detector (FID), which quantified the carbon concentration. After the last temperature ramp in the inert atmosphere a He/O_2 (10%) mixture was introduced into the main oven. In these conditions, additional carbonaceous material was desorbed from the filter and measured through the same process as the OC. To correct for OC pyrolysis, the darkening of the filter was monitored during the analysis by measuring the intensity of light (λ = 660 nm) transmitted through it (Huntzicker et al., 1982). The light transmittance was then used to determine the split point between the PC formed from the OC and the native EC by determining when the transmittance returned to its original value (Turpin et al., 1990, Birch and Cary, 1996).

A machine blank analysis to check for contamination, and analysis of a standard solution (potassium phthalate) to check the accuracy of the system for TC, were performed daily. The blank analysis upper limit was 0.2 µg. The standard solution analysis was not allowed to deviate more than 5% from the expected value.

2.3 Basics of Attenuation Versus Evolved Carbon (AVEC) plots

An AVEC plot relates the attenuation through the filter due to the PM collected on the filter at each second of the analysis to the cumulative carbon evolved during the analysis. Here, attenuation is defined as $ln\ (I_0/I)$ where I_0 is the laser transmittance measured at the end of the analysis when all the carbonaceous compounds were desorbed and I is the transmittance measured at each second of analysis (Haessler, 1965, Ahlquist and Charlson,

1967, Petzold et al., 1997). The cumulative evolved carbon at each second of analysis was calculated from the calibrated, integrated FID signal expressed as mass of carbon per unit area of filter.

Due to the use of $I_{0,}$ the AVEC plot can only be created once the analysis is complete. The R package ggplot2 (Ginestet, 2011) was used to create the AVEC plots from the Rawdata.txt file, as given in the supplement.

3 Results and discussions

This section aims to:

- Present the AVEC plot and compare it to the thermogram.
- Show how the AVEC plot can be used to assess the effect of laser instability on the split between OC and EC.
- Show the importance of the instrument transit time when constructing an AVEC plot and determining the split point in OC/EC analysis more generally.
- Show how the AVEC plot can be a useful tool to spot the presence of early evolution (the removal of dark material during the inert phase) and to evaluate the carbon concentration affected by it.
- Describe how AVEC plots provide information about the optical properties of the particles.
- Compare ambient samples analysed with two protocols, and show the different optical properties among particles from different sites.

3.1 From the thermogram to the AVEC plot: greater clarity of the quantities of carbon and optical changes during the analysis

The OC/EC analysis of a sample is usually visualized in real time by a thermogram, similar to Morita and Rice (1955). Figure 1 shows an example of a thermogram and its corresponding AVEC plot. The thermogram displays the temperature ramps and their starting and ending points; the evolved carbon peaks and their relative abundance; and the laser transmittance signal. Since this information is obtained while the analysis is taking place, thermograms allow anomalous signals to be detected in real time.

In contrast, the AVEC plot shows the properties of the sample rather than the instantaneous instrument sensor status.

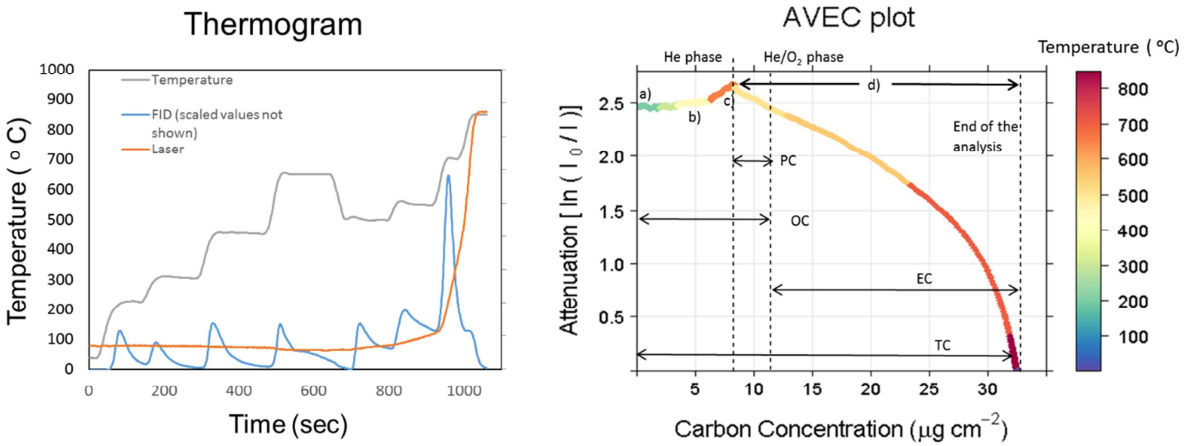

Figure 1. (left) Thermogram showing the FID signal, transmittance intensity, and temperature; (right) corresponding AVEC plot. On the x-axis is the evolved carbon concentration (µg cm^{-2}) and on the y-axis the attenuation ($ln(I_0/I)$); colours indicate the expected sample temperature. The three black dashed lines indicate respectively the change from the inert to oxygenated phases, the split point, and the end of the analysis. The four horizontal arrows directly indicate the OC, PC, EC and TC sample concentrations, as quantified on the x-axis. Both graphs show the analysis of the same sample; a, b, c and d are discussed in the text.

The graph shown on the right of Figure 1 is an AVEC plot of an ambient sample. Again, the analysis proceeds from left to right. The different colours in the AVEC plot represent the changes in temperature, from which it is easy to spot the different carbon fractions that evolved during the analysis. At the beginning of the analysis, the sample deposited on the filter has an attenuation indicated by (a) in the AVEC plot, which would be constant during the inert phase if there were no pyrolysis. However, some organics tend to pyrolyse resulting in an increase in attenuation (b). The attenuation reaches a maximum value at the end of the inert phase (c). The later introduction of O_2 to the main carrier gas results in the removal of dark particles from the sample and a decreasing attenuation (d).

One of the advantages of the AVEC plot is that all the information is summarized in a single line, making it easier to read and interpret. For instance, the AVEC plot can be used to assess the sensitivity of the OC/EC split to the laser instability. Varying the designation of the split point by the estimated laser instability of ±3% (Cavalli et al., 2010) (on the vertical axis in the AVEC plot) allows the corresponding change in OC and EC to be read directly from the horizontal axis. Figure 2 shows that the relative change in OC and EC on the 168 filters for a 3% laser instability, as determined by the gradient of the AVEC plot at the split point. This was different at each monitoring site. The mean change ranged from 7.6% to 14.7% in EC and 0.9% to 18.6% in OC, with greatest sensitivity being displayed by the MY roadside site.

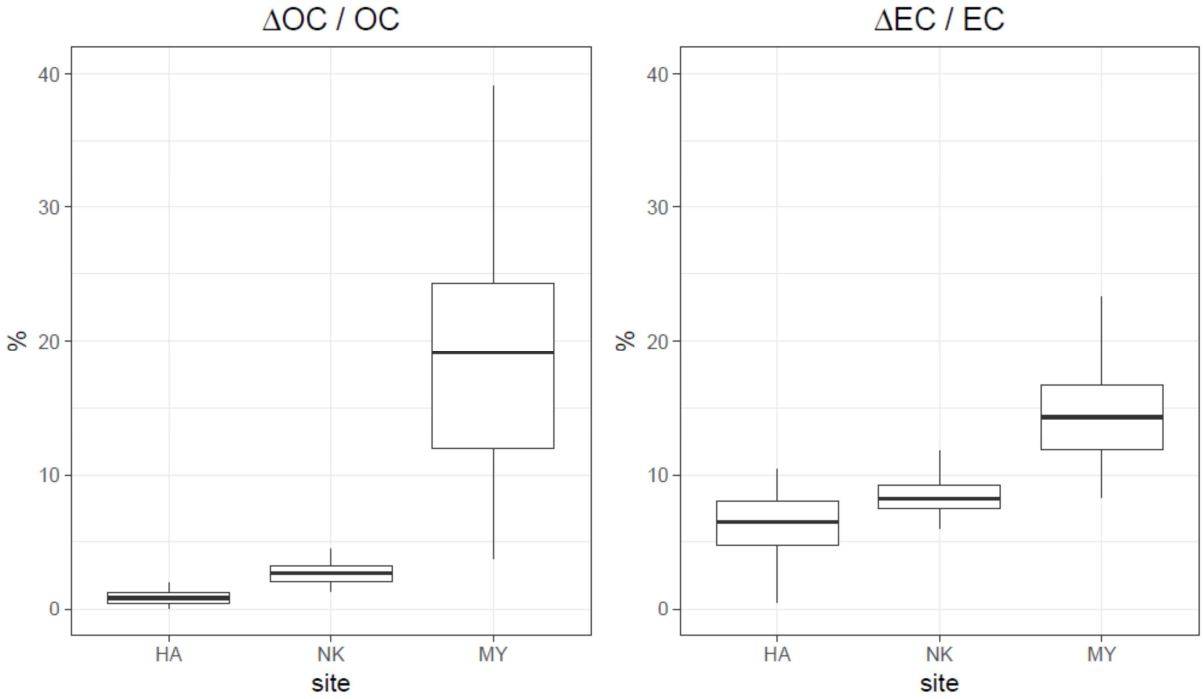

Figure 2. Relative change in OC and EC concentration for each site for a ±3% change in attenuation at the split point for the 168 samples.

Another important benefit of the AVEC plot is that the slope of the curve in the oxygenated phase provides information about the mass absorption cross-section of the material leaving the filter. In the inert gas phase, the gradient does not provide an easily interpretable metric because there are two processes involved: PC formation and OC evolution, rather than just the PC/EC evolution in the oxygenated phase.

Simplistically, if the units on the x-axis are μg cm^{-2}, the gradient of the curve in the oxidising atmosphere region should be the mass absorption cross-section (σ) of the evolving material, expressed in cm^2 μg^{-1} (Liousse et al., 1993). However, this is complicated for reasons similar to those affecting the quantification of mass absorption cross-section within aethalometers or indeed any filter based measurement of light absorption, as discussed in Section 3.4.

3.2 The effect of the instrument transit time on the AVEC plot and the OC /EC split

While the transmittance signal reflects the instantaneous change in the darkening of the sample in the filter, the FID response has a time lag, known as the transit time (Panteliadis et al., 2015). This is the time for the gases evolved from the filter to reach the

FID. Consequently, the attenuation at each second of the analysis does not correspond to the amount of carbon that reaches the detector at that same instant.

Since each instrument differs in model, flow path, etc., the transit time will also differ. The US Environmental Protection Agency (Sarnat et al., 2011) also recommends that a transit time check is performed after any major maintenance.

The transit time is important since it can affect the OC/EC split point assigned by the instrument, and it also influences the gradient of the curve in the oxygenated phase in AVEC plots, and thereby the estimation of σ.

To illustrate this, Figure 3 shows the changes in the AVEC plot using different assumed transit times. The coloured lines represent a range of transit times from 0 (grey line) to 16 seconds (green line). The typical instrumental values of transit time range between 5 and 15 seconds (Panteliadis et al., 2015). For this illustration, a slightly wider range was used, to include the zero value, which refers to the carbon concentration values with no transit time correction. The AVEC curves follow more or less the same path during the first part of the analysis, but diverge in the later part before recombining at the end, when the filter is free of carbonaceous material. The divergence of the plot lines will be noticeable following rapid changes of EC evolution, when an accurate transit time will be important.

Figure 3 shows two samples that exhibit very different properties: in a) the transit time did not significantly affect the determination of the split point; in b) the transit time had a larger effect on the split point. If the divergence of the plot lines is early in the oxygenated phase it affects the split point, otherwise it affects only the determination of optical properties.

The horizontal lines in the plots show different possible split points and the vertical lines indicate the implied OC concentration. In Figure 3 a), only two lines are drawn, one at 0 seconds and the other at 16 seconds transit time. Here, the OC concentration varied by only 3% for the 0-16 second change in transit time. However, the split point was highly influenced by the transit time in Figure 3 b). In this case, the OC concentration varied by 9%, and EC by more than 50% across the different transit time assumptions.

It is noticeable that the gradient of the curve at the end of the ambient sample analysis in Figure 3 changed substantially (from about 0.13 cm^2 μg^{-1} (σ = 13 m^2 g^{-1}) to close to infinite) with the different assumed transit times.

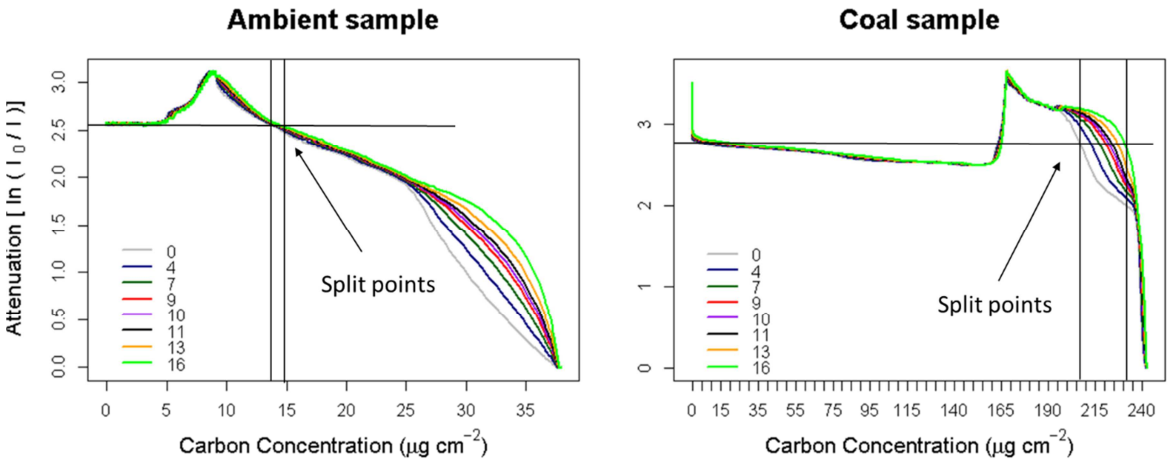

Figure 3. AVEC plots showing the effect of different transit times on the OC/EC split point. The left hand sample is an ambient PM sample and the right hand side is a coal burning emission sample. Vertical lines show split points corresponding to 0 and 16 seconds transit times The AVEC plot colours denote different assumed transit times for each sample.

The impact of transit time assumptions of the analysis split point was tested for all 168 samples. The calculated OC with an assumed transit time of 0 seconds was compared with a transit time of 16 seconds. As shown in Figure 4, the apparent OC increased in all samples with the assumed 16 second transit time, with the corresponding in decrease in EC. The mean bias in OC across the three site types was between 2 and 5 % but a small number of samples had a bias of over 10%. The mean bias in EC was between -4 and -13%. The rural samples showed greater variability.

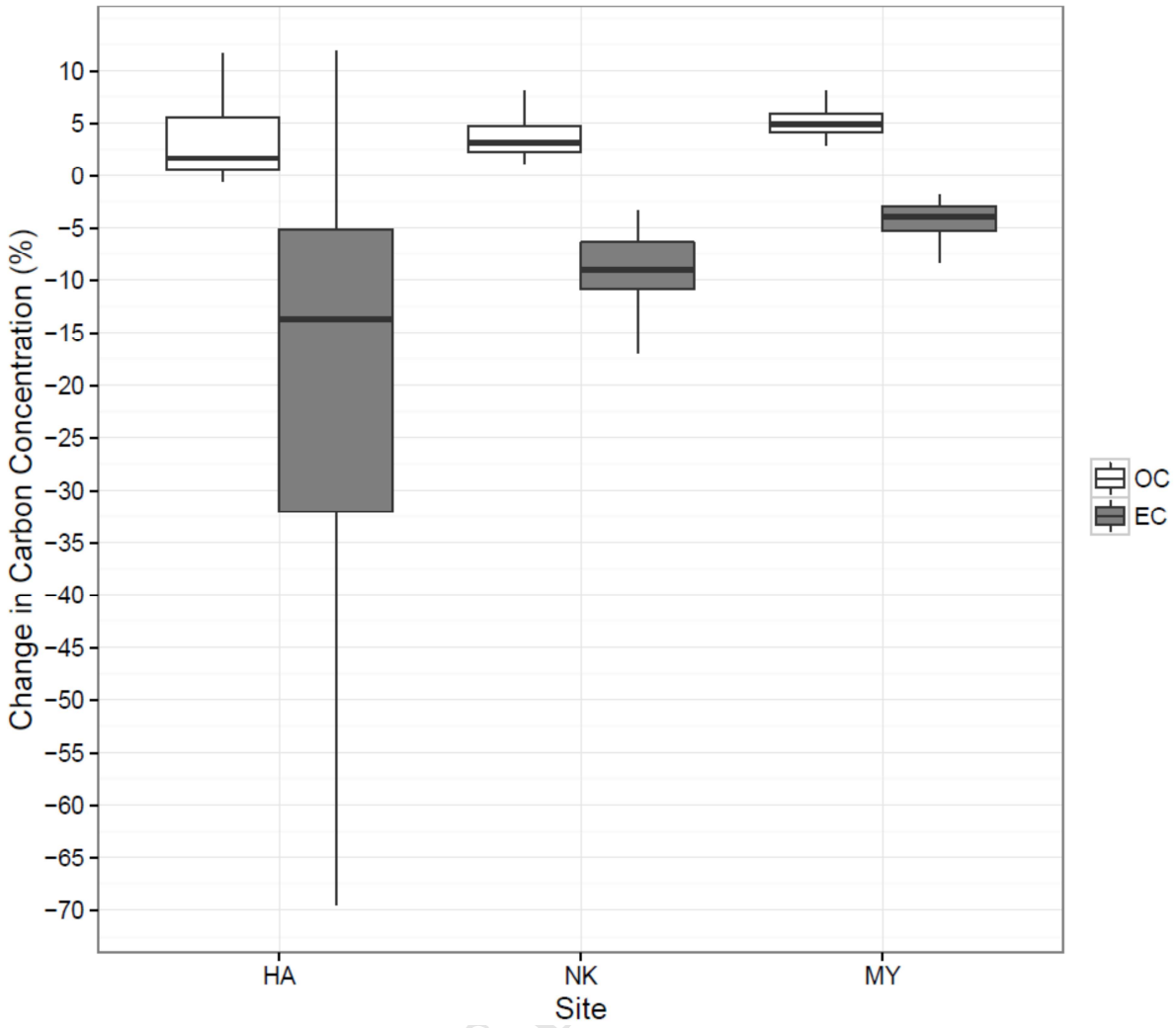

Figure 4 Bias in OC and EC concentration with a transit time of 16 seconds compared with a transit time of zero seconds. HA = Harwell rural, NK = North Kensington background and MY = Marylebone Road kerbside. N = 168.

3.3 Early evolution of EC or PC

Dark particles sometimes evolve during the inert phase when, in principle, only organic carbon (OC) should be leaving the filter. This is termed early evolution (Malm et al., 1994, Yang and Yu, 2002, Yu et al., 2002, Chow et al., 2004, Subramanian et al., 2006). Early evolution occurs when the attenuation decreases during the inert phase of the analysis, meaning that some dark material is desorbed together with the OC.

It is very easy to identify early evolution in the AVEC plot. This happens when the highest point in attenuation precedes the switch of the gas mixture, as in Figure 5.

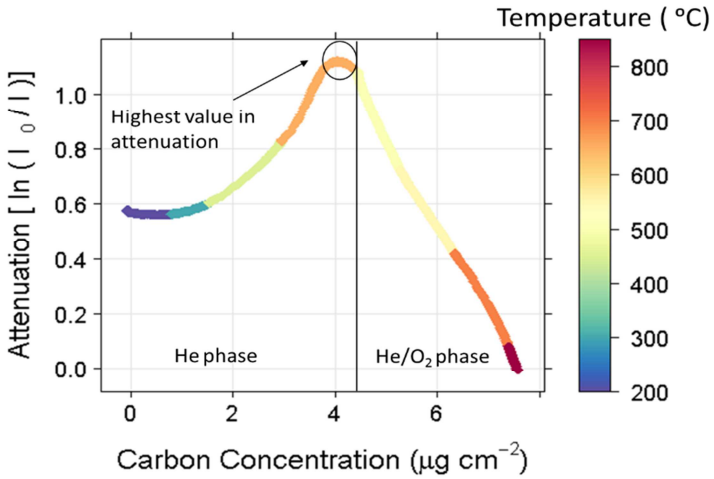

Figure 5. AVEC plot showing early evolution of PC/EC. Circle denotes maximum attenuation and vertical line shows the change from He to He/O_2 atmosphere. The different colours of the curve indicate the temperature changes.

We can have three case scenarios: 1) the dark material evolving is PC, 2) it is EC or 3) it is a mixture of the two. If it is PC that evolved in the inert phase, it does not affect the OC/EC split because this was OC that underwent pyrolysis. Moreover, the assigned split point would be unaffected because it takes into account the attenuation at the beginning of the analysis and not at the highest value. However, if the particles evolving in the inert phase are native EC, early evolution would affect the determination of OC and EC concentrations, but only if the σ of PC and EC differs. If σ of EC is smaller than PC we would have an overestimation of OC and vice versa. If it is a mix of the two it would interfere with the analysis only if the PC and EC on the filter have different σ.

Early evolution occurred in 47 out of 168 samples (28%) analysed with EUSAAR_2 protocol and in 105 out of 160 samples (65%) analysed following the Quartz protocol.

3.4 Quantitative optical information from AVEC plots

If the area of the filter is well defined and the entire light beam passes through the sample, then a value for the mass absorption cross-section (σ) of the material leaving the filter in the oxygenated phase can be obtained directly from the AVEC plot. The slope of this section of the curve is given by (Liousse et al., 1993):

$$\frac{\Delta \text{Attenuation}}{\Delta Carbon\ evolved} = \sigma \qquad \text{(Equation 1)}$$

Given that the y-axis of the AVEC plot is optical attenuation and the x-axis is the carbon evolved up in the oxygenated phase (in μg cm^{-2}), the gradient of the curve in the oxygenated phase is in principle the mass absorption cross-section of the evolving material, in units of cm^2 μg^{-1}. This can be multiplied by 100 to give the more usual units of m^2 g^{-1}.

However, the determination of the mass absorption cross-section has some caveats. Similar to an aethalometer or particle soot absorption photometer, the change in attenuation will be determined by the mass absorption cross-section of the material leaving the filter but also by some artefacts such as multiple scattering within the filter, undetected scattered light, and shadowing (Gundel et al., 1984, Petzold et al., 1997, Weingartner et al., 2003, Arnott et al., 2005, Davy et al., 2017). These change the apparent mass absorption cross-section and partially depend on the amount of dark material on the filter. Undetected scattered light depends on the geometry of the light source, filter and light sensor (Vecchi et al., 2014). Due to the relatively large separation of the light source and sensor in an OCEC instrument compared, for example, with an aethalometer, this type of scattering would be expected to play a more significant role. Generally, lower mass absorption cross-sections are measured with highly loaded filters compared to lightly loaded ones because of shadowing. This widely recognised non-linearity between the apparent mass absorption cross-section and the amount of dark material on a filter is often approximated as a quadratic function (Virkkula et al., 2007, Park et al., 2010, Davy et al., 2017). Nevertheless, notable changes in absorption cross-section of the material evolved at different stages of the analysis should be relevant to the PC/EC question and to source apportionment.

At the start of the oxygenated atmosphere phase, the material on the filter will be the original EC along with any pyrolysed material, and in principle it could be possible to distinguish between the two using the AVEC curve. In thermal-optical analyses, the accurate discrimination between OC and EC relies upon either one or the other of the following two assumptions being true: 1) PC formed during the He-mode is assumed to have the same σ as the native atmospheric EC (Moosmüller et al., 2009). If so, regardless of when PC and EC actually evolve from the filter during the analysis, the desorbed carbon beyond the split point is equivalent to the amount of native EC. 2) Alternatively, all PC formed during the He-phase is assumed to evolve from the filter before the native EC. In this case, despite possible differences in σ of PC and EC, the post-split point carbon still represents the true native EC. Previous studies (Yang and Yu, 2002, Yu et al., 2002, Subramanian et al., 2006) showed that these assumptions are not always valid. PC and EC have been found to co-evolve during the He/O_2-phase and, even, prematurely from the He-phase at high temperatures (as shown in Figure 5); moreover, they have been shown to have significantly different values of σ (Yang and Yu, 2002, Yu et al., 2002, Chow et al., 2004, Subramanian et al., 2006, Han et al., 2007). There are, then, inherent potential biases in both directions in the determination of OC and EC. Subramanian et al. (2006) suggest that original EC is less dark than the pyrolysed

material. If less dark original EC is evolved first, the split point will come too late, the estimated pyrolysed material will be too large and EC will be measured as too low (Karanasiou et al., 2015). Conversely, if original EC is darker than the pyrolysed material and evolves first then the split point will be too soon and the bias in the OC/EC split will be reversed.

In contrast to thermograms, the AVEC plot provides a means to examine the mass absorption cross-section of material leaving the filter at different stages of the analysis to investigate the validity of the assumptions affecting the OC/EC split.

There are clear differences in the AVEC plots of the samples shown in Figure 1 and Figure 3a and the coal sample shown in Figure 3b. The carbon evolving from the middle stages of the oxygenated phase in the coal sample is much less absorbing than the material evolving from the same stage with the ambient samples. This would be consistent with concepts of black and brown carbon in this coal emission sample (Andreae and Gelencsér, 2006, Reisinger et al., 2008). Alternatively, this could be due to different mass absorption cross sections and evolution temperatures for the native elemental and pyrolysed carbon in this sample.

When absorption is measured with the intention to derive "black carbon" concentrations, a measured or assumed specific value of σ must be used to convert light absorption to mass concentration of EC. In the conventional measurement of black carbon by aethalometer, a relationship between black carbon concentration and light attenuation uses value of σ of 16.6 m^2 g^{-1}. Davy et al. (2017) showed that on-filter values of σ are filter-material dependent. Great care must be taken when comparing values reported for σ because of the associated artefacts (Vecchi et al., 2014, Davy et al., 2017).

For particles deposited on quartz filters, literature values of σ for native EC range from 8.1 m^2 g^{-1} to 25.4 m^2 g^{-1} for solvent-extracted ambient samples (Gundel et al., 1984, Liousse et al., 1993, Petzold et al., 1997, Subramanian et al., 2006). The reported values of σ for PC are almost always greater: in particular, 35 m^2 g^{-1} was found for Pittsburgh samples (Subramanian et al., 2006), 52.8 ± 10.6 m^2 g^{-1} (average ± standard deviation) for Fresno samples and 48.5 ± 3.9 m^2 g^{-1} was reported for IMPROVE network samples (Chow et al., 2004). Davy et al. (2017) found that σ values vary by filter type and found values 72 ± 19 m^2 g^{-1} for quartz filters.

These values can be compared with those derived from AVEC plots for ambient samples in the next section.

3.5 Ambient samples analysed by EUSAAR_2 and Quartz protocols

In this section, AVEC plots were used to investigate the differences in optical properties among particles from different ambient environments, and the effect of the protocol on the PC formation.

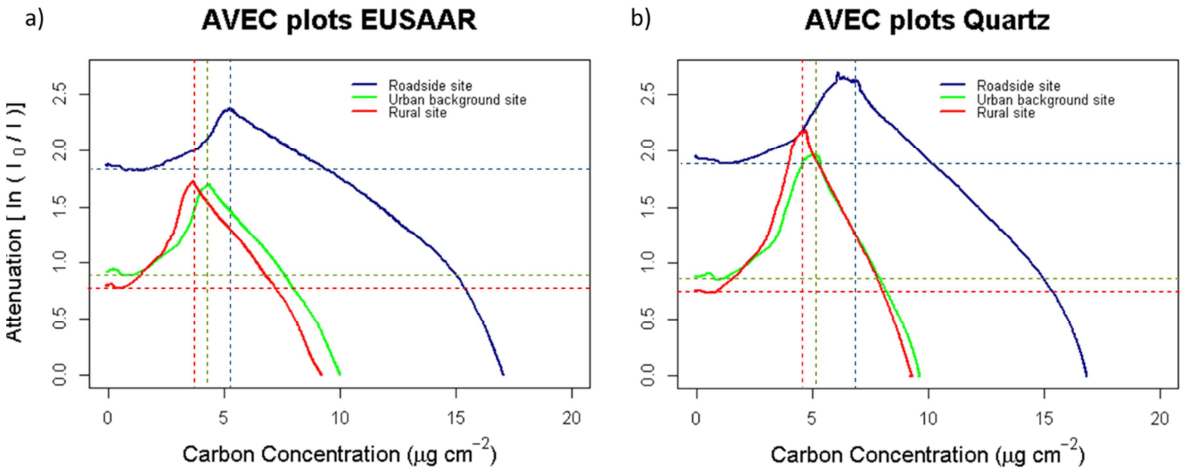

Figure 6. AVEC plots of urban background (North Kensington, in green), rural (Harwell, in red) and roadside (Marylebone Road, in navy) ambient samples analysed with EUSAAR_2 (a) and Quartz (b) protocols. These protocols are set out in the Supplementary Information. The change in atmosphere is indicated with the vertical dashed line and horizontal dashed lines denotes the attenuation at the start of the sample analysis.

As shown in Figure 6, the urban and rural samples had similar initial attenuation and total carbon concentration, while the roadside sample had twice the initial attenuation of the urban and rural samples and slightly less than twice the total carbon concentration. The initial attenuation value of each sample and the total carbon agreed within 5% for the two protocols.

Figure 7 shows the AVEC plots from the three ambient samples shown in Figure 6, highlighting the PC formation and correction. The EUSAAR_2 and Quartz analyses show a similar amount of pyrolysis in terms of concentration of PC determined by the instrument, indicated by the base of the triangles. However, the change in attenuation due to pyrolysis, indicated by the height of the triangles, was significantly greater in the Quartz analyses. The Quartz protocol shows greater darkening of the sample in the inert phase. The differences in gradient of the hypotenuse of the triangles indicate that material with different optical properties was evolved at the beginning of the oxidised phase in the two protocols. The PC formed in the higher temperature Quartz protocol had greater σ than that formed in the EUSAAR_2 protocol.

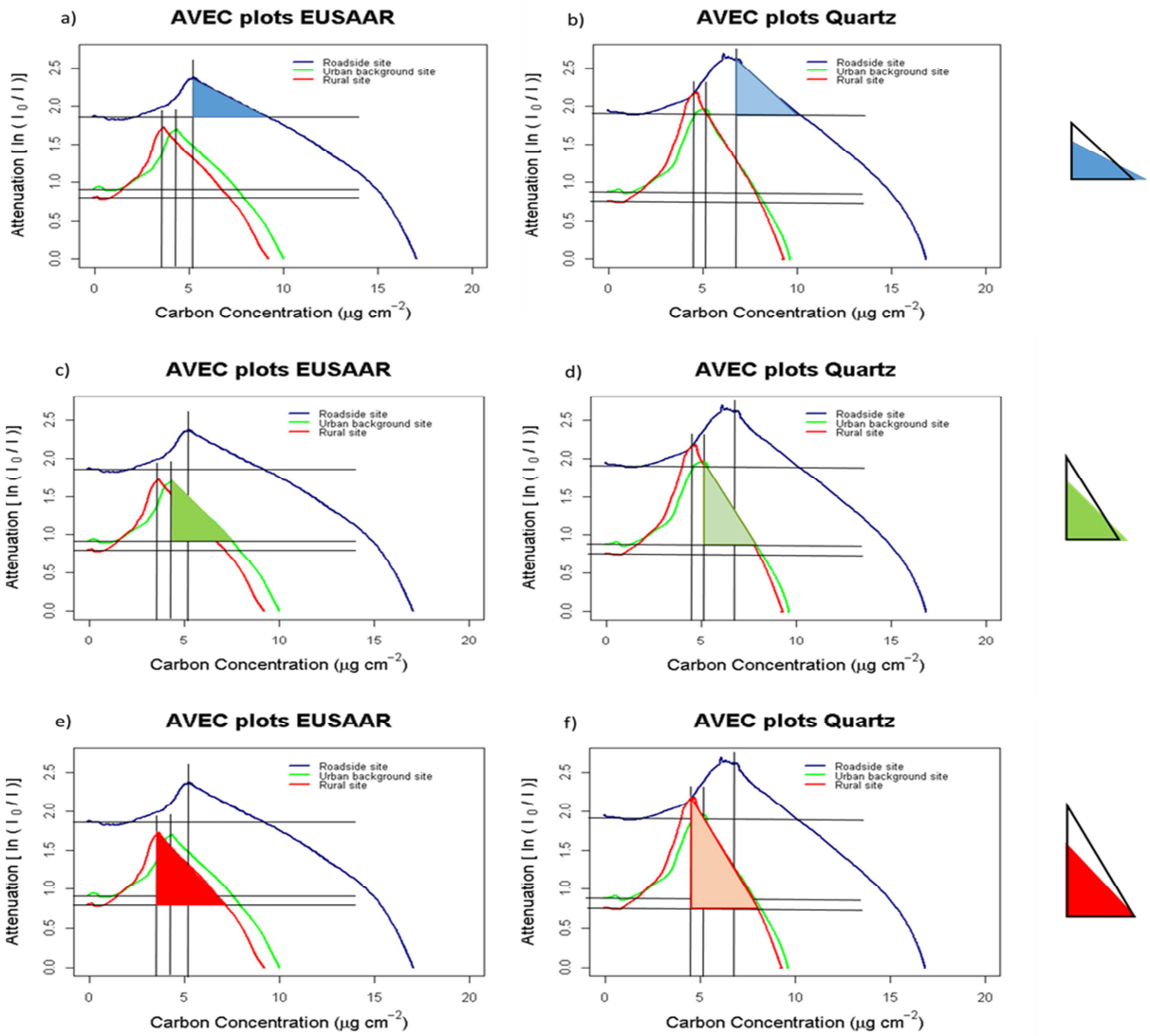

407

408 Figure 7. AVEC plots of ambient samples from urban (North Kensington), rural (Harwell) and
409 roadside (Marylebone Road) sites analysed with the EUSAAR_2 (a, c, e) and the Quartz (b, d,
410 f) protocols. The change in atmosphere is indicated with the vertical black line. The coloured
411 triangles inside the AVEC plots indicate the area in the oxygenated phase that corresponds
412 to the PC correction. The triangles to the right of the plots show the differences in the
413 gradients and areas between the sample analysed with EUSAAR_2 (coloured) and Quartz
414 (the transparent triangle with black border line).

415

416 To assess the correlation between attenuation increase in the inert phase and PC
417 concentration, 149 ambient samples from the three sites were analysed using the two
418 protocols and plotted against each other. Correlations were calculated using Reduced Major
419 Axis (RMA) (Ayers (2001); Warton et al. (2006). The attenuation increase during the inert
420 phase is about 25% lower in the samples analysed using the EUSAAR_2 protocol compared
421 to the Quartz one (Figure 8a; slope = 0.75 ± 0.04; intercept: -0.01 ± 0.03; R = 0.95). However,
422 the values of PC derived from the EUSAAR_2 protocol were 10% higher compared to the

ones calculated from the Quartz one (Figure 8b; slope: = 1.10 ± 0.03; intercept: 0.22 ± 0.12; R=0.98). This is in agreement with the earlier observation that the material evolving at the beginning of the oxygenated phase in the Quartz samples had, on average, higher σ than the EUSAAR_2 ones.

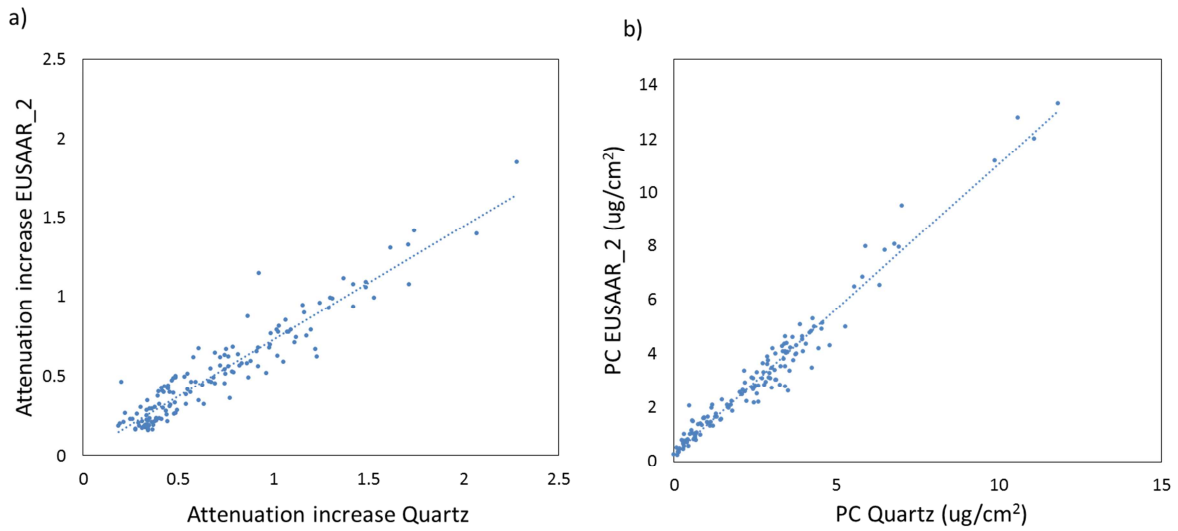

Figure 8. Correlation of the attenuation increase due to pyrolysis (a) and concentrations of PC (b) as observed from 149 ambient samples analysed using both the EUSAAR_2 and the Quartz protocols.

Average apparent σ values were calculated for the ambient samples analysed using the EUSAAR_2 protocol using Equation (1). The attenuation change was calculated as the difference between the attenuation measured at the start of the oxygenated phase and the attenuation at the end of the analysis; and the carbon evolved was the sum of PC and EC concentrations. We found a range of σ of 30 ± 6 $m^2 g^{-1}$ in rural samples, 23 ± 6 $m^2 g^{-1}$ in urban samples and 12 ± 3.5 $m^2 g^{-1}$ in roadside samples. The roadside samples had lowest σ probably because they were most influenced by the shadowing effect. To avoid the shadowing effect we measured the slope of the curve in the area close to the end of the analysis, where it should not affect the analysis due to the small content of carbon remaining. The σ measured in this section of the curve had similar values to the σ values found for the PC reported in the literature: 45 ± 10 $m^2 g^{-1}$ (rural samples); 42 ± 8 $m^2 g^{-1}$ (urban samples); and 35 ± 14 $m^2 g^{-1}$ (roadside samples).

4 Conclusions

AVEC plots are a new visual representation of the behaviour of a sample during OCEC analysis. They are complementary to thermograms, which focus on the instrument outputs

rather than the sample properties. One of the advantages of using the AVEC plot is that it is possible to evaluate the amount of pyrolysis, OC, PC, and EC directly from the graph.

The AVEC plot highlights how laser instability and the assumed instrument transit time can affect the attribution of OC, PC, and EC, and how an erroneous transit time value can affect the estimation of σ in the oxygenated phase. Furthermore, the AVEC plot is a useful tool to identify if any early evolution is occurring and estimate the amount of carbon involved.

However, the most important feature of this plot is that the gradient of the curve in the oxygenated phase indicates the σ of the particles deposited on the filter. This information can be used to improve the reliability of the split point between OC and EC, and to investigate the optical properties of the material on the filter. For example, clear differences were seen in the AVEC plots between coal emission and ambient samples. For full quantitative information it is necessary to account for artefacts, such as the shadowing effect and the effects of scattered light. The shadowing effect, due to a large quantity of particles deposited on the filter, causes an underestimation of the measured attenuation and of the calculated σ in the same way as for an aethalometer. Another important factor to account for is the geometry of the instrument. If the detector is too far from the sample it can miss scattered light leading to an overestimation of the measured attenuation.

The average apparent σ values calculated in the oxygenated phase of the ambient samples were comparable to that found in the literature. The roadside site sample showed lower average σ than the other samples, presumably due to a larger shadowing effect. The σ values calculated from the later part of the oxygenated phase curve, which should minimise shadowing effects, gave consistent results among the different sites.

Furthermore, the AVEC plots presented here highlight that the optical properties of the PC formed during the analysis varies by protocol. The PC formed by the higher temperature Quartz protocol had a greater σ than that produced by the lower temperature EUSAAR_2 protocol. The AVEC plots show that these differences were evident in the carbon evolving at the beginning of the oxygenated phase. Therefore, we conclude that in these cases PC evolved at lower temperatures than the native EC in ambient samples. This could explain the systematic 10% difference observed between the PC measured by the two protocols. However, shadowing effects prevent the determination of an artefact free σ from the upper part of AVEC curve and at present the assumptions of Yang and Yu, 2002 cannot yet be tested.

5 Acknowledgements

This work was funded by The Engineering and Physical Sciences Research Council (EPSRC) studentship (PO:420898).

The authors are also grateful to Professor John Wenger and team at the University College Cork for providing solid fossil fuel samples and to the Irish Environmental Protection Agency for funding these collections as part of the Sapphire project.

6 References

AHLQUIST, N. C. & CHARLSON, R. J. 1967. A new instrument for evaluating the visual quality of air. *Journal of the Air Pollution Control Association,* 17**,** 467-469.

ANDREAE, M. & GELENCSÉR, A. 2006. Black carbon or brown carbon? The nature of light-absorbing carbonaceous aerosols. *Atmospheric Chemistry and Physics,* 6**,** 3131-3148.

ARNOTT, W. P., HAMASHA, K., MOOSMÜLLER, H., SHERIDAN, P. J. & OGREN, J. A. 2005. Towards aerosol light-absorption measurements with a 7-wavelength aethalometer: Evaluation with a photoacoustic instrument and 3-wavelength nephelometer. *Aerosol Science and Technology,* 39**,** 17-29.

ATKINSON, R. W., ANALITIS, A., SAMOLI, E., FULLER, G. W., GREEN, D. C., MUDWAY, I. S., ANDERSON, H. R. & KELLY, F. J. 2015. Short-term exposure to traffic-related air pollution and daily mortality in London, UK. *Journal of Exposure Science and Environmental Epidemiology*.

AYERS, G. 2001. Comment on regression analysis of air quality data. *Atmospheric Environment,* 35**,** 2423-2425.

BIRCH, M. & CARY, R. 1996. Elemental carbon-based method for monitoring occupational exposures to particulate diesel exhaust. *Aerosol Science and Technology,* 25**,** 221-241.

BUTTERFIELD, D., BECCACECI, S., QUINCEY, P., LILLEY, A., BRADSHAW, C., FULLER, G., GREEN, D. & FONT FONT, A. 2013. NPL Report AS 92: 2013 Annual Report for the UK Black Carbon Network. *NPL, Teddington*.

CACHIER, H., BREMOND, M. P. & BUAT-MÉNARD, P. 1989. Determination of atmospheric soot carbon with a simple thermal method. *Tellus B,* 41**,** 379-390.

CAVALLI, F., VIANA, M., YTTRI, K. E., GENBERG, J. & PUTAUD, J.-P. 2010. Toward a standardised thermal-optical protocol for measuring atmospheric organic and elemental carbon: the EUSAAR protocol. *Atmospheric Measurement Techniques,* 3**,** 79-89.

CHIAPPINI, L., VERLHAC, S., AUJAY, R., MAENHAUT, W., PUTAUD, J., SCIARE, J., JAFFREZO, J., LIOUSSE, C., GALY-LACAUX, C. & ALLEMAN, L. 2014. Clues for a standardised thermal-optical protocol for the assessment of organic and elemental carbon within ambient air particulate matter. *Atmospheric Measurement Techniques,* 7**,** 1649-1661.

CHOW, J. C., WATSON, J. G., CHEN, L.-W. A., ARNOTT, W. P., MOOSMÜLLER, H. & FUNG, K. 2004. Equivalence of elemental carbon by thermal/optical reflectance and transmittance with different temperature protocols. *Environmental science & technology,* 38**,** 4414-4422.

CHOW, J. C., WATSON, J. G., CHEN, L.-W. A., CHANG, M. O., ROBINSON, N. F., TRIMBLE, D. & KOHL, S. 2007. The IMPROVE_A temperature protocol for thermal/optical carbon analysis: maintaining consistency with a long-term database. *Journal of the Air & Waste Management Association,* 57**,** 1014-1023.

DAVY, P. M., TREMPER, A. H., NICOLOSI, E. M., QUINCEY, P. & FULLER, G. W. 2017. Estimating particulate black carbon concentrations using two offline light absorption methods applied to four types of filter media. *Atmospheric Environment*.

DIRECTIVE 2008. Council Directive 2008/50/EC on ambient air and cleaner air for Europe. *Official Journal of the European Communities,* L151, 1e44

FUNG, K., CHOW, J. C. & WATSON, J. G. 2002. Evaluation of OC/EC speciation by thermal manganese dioxide oxidation and the IMPROVE method. *Journal of the Air & Waste Management Association,* 52**,** 1333-1341.

GINESTET, C. 2011. ggplot2: elegant graphics for data analysis. *Journal of the Royal Statistical Society: Series A (Statistics in Society),* 174**,** 245-246.

GUNDEL, L., DOD, R., ROSEN, H. & NOVAKOV, T. 1984. The relationship between optical attenuation and black carbon concentration for ambient and source particles. *Science of the Total Environment,* 36**,** 197-202.

HAESSLER, W. M. 1965. Smoke detection by forward light scattering. *Fire Technology,* 1**,** 43-51.

HAN, Y., CAO, J., CHOW, J. C., WATSON, J. G., AN, Z., JIN, Z., FUNG, K. & LIU, S. 2007. Evaluation of the thermal/optical reflectance method for discrimination between char-and soot-EC. *Chemosphere,* 69**,** 569-574.

HITZENBERGER, R., PETZOLD, A., BAUER, H., CTYROKY, P., POURESMAEIL, P., LASKUS, L. & PUXBAUM, H. 2006. Intercomparison of thermal and optical measurement methods for elemental carbon and black carbon at an urban location. *Environmental science & technology,* 40**,** 6377-6383.

HUNTZICKER, J., JOHNSON, R., SHAH, J. & CARY, R. 1982. Analysis of organic and elemental carbon in ambient aerosols by a thermal-optical method. *Particulate Carbon.* Springer.

IPCC Intergovernmental Panel on Climate Change. Climate Change 2013: The Physical Science Basis. Contribution of Working Group I to the Fifth Assessment Report of the Intergovernmental Panel on Climate Change. *Cambridge University Press: Cambridge, U.K. and New York, U.S.A.,* 2013.

JACOBSON, M. Z. 2010. Short-term effects of controlling fossil-fuel soot, biofuel soot and gases, and methane on climate, Arctic ice, and air pollution health. *Journal of Geophysical Research: Atmospheres,* 115.

JANSSEN, N. A., GERLOFS-NIJLAND, M. E., LANKI, T., SALONEN, R. O., CASSEE, F., HOEK, G., FISCHER, P., BRUNEKREEF, B. & KRZYZANOWSKI, M. 2012. *Health effects of black carbon*, WHO Regional Office for Europe Copenhagen.

JANSSEN, N. A., HOEK, G., SIMIC-LAWSON, M., FISCHER, P., VAN BREE, L., TEN BRINK, H., KEUKEN, M., ATKINSON, R. W., ANDERSON, H. R. & BRUNEKREEF, B. 2011. Black Carbon as an Additional Indicator of the Adverse Health Effects of Airborne Particles Compared with PM^ sub 10^ and PM^ sub 2.5. *Environmental Health Perspectives,* 119**,** 1691.

KARANASIOU, A., MINGUILLÓN, M. C., VIANA, M., ALASTUEY, A., PUTAUD, J.-P., MAENHAUT, W., PANTELIADIS, P., MOČNIK, G., FAVEZ, O. & KUHLBUSCH, T. A. 2015. Thermal-optical analysis for the measurement of elemental carbon (EC) and organic carbon (OC) in ambient air a literature review.

KIM, K.-H., KABIR, E. & KABIR, S. 2015. A review on the human health impact of airborne particulate matter. *Environment International,* 74**,** 136-143.

LENA, T. S., OCHIENG, V., CARTER, M., HOLGUÍN-VERAS, J. & KINNEY, P. L. 2002. Elemental carbon and PM (2.5) levels in an urban community heavily impacted by truck traffic. *Environmental Health Perspectives,* 110**,** 1009.

LIOUSSE, C., CACHIER, H. & JENNINGS, S. 1993. Optical and thermal measurements of black carbon aerosol content in different environments: Variation of the specific attenuation cross-section, sigma (σ). *Atmospheric Environment. Part A. General Topics,* 27**,** 1203-1211.

MALM, W. C., SISLER, J. F., HUFFMAN, D., ELDRED, R. A. & CAHILL, T. A. 1994. Spatial and seasonal trends in particle concentration and optical extinction in the United States. *Journal of Geophysical Research: Atmospheres,* 99**,** 1347-1370.

MOOSMÜLLER, H., CHAKRABARTY, R. & ARNOTT, W. 2009. Aerosol light absorption and its measurement: A review. *Journal of Quantitative Spectroscopy and Radiative Transfer,* 110**,** 844-878.

583 MORITA, H. & RICE, H. 1955. Characterization of Organic Substances by Differential Thermal
584 Analysis: General Experimental Technique. *Analytical Chemistry,* 27**,** 336-339.
585 PANTELIADIS, P., HAFKENSCHEID, T., CARY, B., DIAPOULI, E., FISCHER, A., FAVEZ, O., QUINCEY, P.,
586 VIANA, M., HITZENBERGER, R. & VECCHI, R. 2015. ECOC comparison exercise with identical
587 thermal protocols after temperature offset correction: instrument diagnostics by in-depth
588 evaluation of operational parameters. *Atmospheric Measurement Techniques,* 8**,** 779-792.
589 PARK, S. S., HANSEN, A. D. & CHO, S. Y. 2010. Measurement of real time black carbon for
590 investigating spot loading effects of Aethalometer data. *Atmospheric Environment,* 44**,** 1449-
591 1455.
592 PETZOLD, A., KOPP, C. & NIESSNER, R. 1997. The dependence of the specific attenuation cross-
593 section on black carbon mass fraction and particle size. *Atmospheric Environment,* 31**,** 661-
594 672.
595 PETZOLD, A., OGREN, J. A., FIEBIG, M., LAJ, P., LI, S.-M., BALTENSPERGER, U., HOLZER-POPP, T.,
596 KINNE, S., PAPPALARDO, G. & SUGIMOTO, N. 2013. Recommendations for reporting" black
597 carbon" measurements. *Atmospheric Chemistry and Physics,* 13**,** 8365-8379.
598 QADIR, R., ABBASZADE, G., SCHNELLE-KREIS, J., CHOW, J. & ZIMMERMANN, R. 2013. Concentrations
599 and source contributions of particulate organic matter before and after implementation of a
600 low emission zone in Munich, Germany. *Environmental pollution,* 175**,** 158-167.
601 RAMANATHAN, V. & CARMICHAEL, G. 2008. Global and regional climate changes due to black
602 carbon. *Nature geoscience,* 1**,** 221-227.
603 REISINGER, P., WONASCHÜTZ, A., HITZENBERGER, R., PETZOLD, A., BAUER, H., JANKOWSKI, N.,
604 PUXBAUM, H., CHI, X. & MAENHAUT, W. 2008. Intercomparison of measurement techniques
605 for black or elemental carbon under urban background conditions in wintertime: Influence
606 of biomass combustion. *Environmental science & technology,* 42**,** 884-889.
607 SAMOLI, E., ATKINSON, R. W., ANALITIS, A., FULLER, G. W., GREEN, D. C., MUDWAY, I., ANDERSON,
608 H. R. & KELLY, F. J. 2016. Associations of short-term exposure to traffic-related air pollution
609 with cardiovascular and respiratory hospital admissions in London, UK. *Occupational and*
610 *environmental medicine***,** oemed-2015-103136.
611 SARNAT, J., DATE, M. K., DATE, G. Z., DATE, K. H., DATE, P. T. & DATE, T. R. 2011. Quality Assurance
612 Project Plan for Project 2 EPA Clean Air Research Center.
613 SCHAUER, J. J., MADER, B., DEMINTER, J., HEIDEMANN, G., BAE, M., SEINFELD, J. H., FLAGAN, R.,
614 CARY, R., SMITH, D. & HUEBERT, B. 2003. ACE-Asia intercomparison of a thermal-optical
615 method for the determination of particle-phase organic and elemental carbon.
616 *Environmental science & technology,* 37**,** 993-1001.
617 SUBRAMANIAN, R., KHLYSTOV, A. Y. & ROBINSON, A. L. 2006. Effect of peak inert-mode temperature
618 on elemental carbon measured using thermal-optical analysis. *Aerosol Science and*
619 *Technology,* 40**,** 763-780.
620 TURPIN, B. J., CARY, R. & HUNTZICKER, J. 1990. An in situ, time-resolved analyzer for aerosol organic
621 and elemental carbon. *Aerosol Science and Technology,* 12**,** 161-171.
622 VECCHI, R., BERNARDONI, V., PAGANELLI, C. & VALLI, G. 2014. A filter-based light-absorption
623 measurement with polar photometer: Effects of sampling artefacts from organic carbon.
624 *Journal of Aerosol Science,* 70**,** 15-25.
625 VIRKKULA, A., MÄKELÄ, T., HILLAMO, R., YLI-TUOMI, T., HIRSIKKO, A., HÄMERI, K. & KOPONEN, I. K.
626 2007. A simple procedure for correcting loading effects of aethalometer data. *Journal of the*
627 *Air & Waste Management Association,* 57**,** 1214-1222.
628 WARTON, D. I., WRIGHT, I. J., FALSTER, D. S. & WESTOBY, M. 2006. Bivariate line-fitting methods for
629 allometry. *Biological Reviews,* 81**,** 259-291.
630 WATSON, J. G., CHOW, J. C. & CHEN, L.-W. A. 2005. Summary of organic and elemental carbon/black
631 carbon analysis methods and intercomparisons. *Aerosol Air Qual. Res,* 5**,** 65-102.

632 WEINGARTNER, E., SAATHOFF, H., SCHNAITER, M., STREIT, N., BITNAR, B. & BALTENSPERGER, U.
633 2003. Absorption of light by soot particles: determination of the absorption coefficient by
634 means of aethalometers. *Journal of Aerosol Science,* 34**,** 1445-1463.
635 YANG, H. & YU, J. Z. 2002. Uncertainties in charring correction in the analysis of elemental and
636 organic carbon in atmospheric particles by thermal/optical methods. *Environmental science*
637 *& technology,* 36**,** 5199-5204.
638 YU, J. Z., XU, J. & YANG, H. 2002. Charring characteristics of atmospheric organic particulate matter
639 in thermal analysis. *Environmental science & technology,* 36**,** 754-761.

640 ZHANG, R., WANG, G., GUO, S., ZAMORA, M. L., YING, Q., LIN, Y., WANG, W., HU, M. & WANG, Y.
641 2015. Formation of urban fine particulate matter. *Chemical reviews,* 115**,** 3803-3855.

642

Light attenuation versus evolved carbon (AVEC) – a new way to look at elemental and organic carbon analysis

E.M.G. Nicolosi, P. Quincey, A. Font and G.W. Fuller

Highlights

We provide a new way to represent thermal-optical OC/EC analysis data (AVEC plot).

The AVEC plot focuses on the sample properties, not the instrument sensor status.

It allows the investigation of the optical properies of carbon particles.

The optical properties of pyrolysed ambient carbon differed between protocols.